J. Fluid Mech. (1994), vol. 270, pp. 199–217

The non-Gaussian statistics of the velocity field in low-resolution large-eddy simulations of homogeneous turbulence

By MARCO BRISCOLINI AND PAOLO SANTANGELO

IBM ECSEC, European Center for Scientific and Engineering Computing,
Viale Oceano Pacifico, 171, 00144 Roma, Italy

(Received 18 August 1992 and in revised form 3 January 1994)

A low-resolution (64^3) large-eddy model of forced homogeneous turbulence is numerically simulated using Kraichnan's eddy viscosity. The introduction of a reliable statistical estimate of the ζ_p exponents allows one to perform a detailed statistical analysis of the velocity field and shows that the probability distribution functions, the structure functions and the power-law exponents ζ_p agree with previous numerical and experimental results obtained at much higher effective resolution. This result shows how a simple modelling of the energy transfer produces self-similar dynamics extending to the small scales and obtains the right statistical properties of the velocity field.

1. Introduction

Experimental measurements (Antonia *et al.* 1982; Anselmet *et al.* 1984; Meneveau & Sreenivasan 1987*a*; Castaigne *et al.* 1990; Meneveau & Sreenivasan 1991) and direct numerical simulations (Kerr 1985; Hosokawa & Yamamoto 1990; Vincent & Meneguzzi 1991; Kida & Ohkitani 1992) of three-dimensional turbulent flows have clearly shown how the self-similar energy cascade occurs through the repeated fragmentation of the vorticity field and how this process generates elongated spatial structures (vorticity tubes) which form a fractal set where dissipation eventually takes place. This physical mechanism contrasts with Kolmogorov's early theory (Kolmogorov 1941) of homogeneous turbulence (hereafter referred to as K41) where the self-similar energy cascade was considered as a continuous and not intermittent phenomenon, which originated uniformly distributed dissipative structures.

In order to take into account the experimental evidence of a strong space-temporal intermittency of the turbulent field, different models of the energy cascade have been proposed as corrections to the basic K41 theory. Among these, the most popular theories are: (i) the Kolmogorov–Obukhov log-normal theory (Obukhov 1962; Kolmogorov 1962; Monin & Yaglom 1975), which is an attempt to describe the spatial intermittency of the energy dissipation; (ii) Mandelbrot's fractal model (Mandelbrot 1974), where the dissipative structures are supposed to belong to a fractal set; and (iii) the β-model (Frisch *et al.* 1978) where the intermittent energy cascade is described by a more phenomenological approach while retaining the basic standard fractal hypothesis about the dissipation field.

All the theories of intermittency in turbulence are characterized by a parameter, the intermittency coefficient μ, which appears in the expression for the high-order statistics

of the velocity differences, namely the velocity structure functions, $\langle|\delta u_x(r)|^p\rangle = \int |\delta u_x(r)|^p P(\delta u_x(r))\,\mathrm{d}\delta u_x(r)$ (where $P(\delta u_x(r)) = P(u_x(\boldsymbol{x}+\boldsymbol{r}) - u_x(\boldsymbol{x}))$ is the probability distribution function, hereafter referred to as PDF, of the velocity difference at scale r). The basic hypothesis of all these theories is that the structure functions $\langle|\delta u_x(r)|^p\rangle$ scale as r^{ζ_p} where the ζ_p exponent is

$$\zeta_p = \frac{1}{3}p - \frac{1}{18}\mu p(p-3) \tag{1.1}$$

for the Kolmogorov–Obukhov log-normal model and is

$$\zeta_p = \frac{1}{3}p - \frac{1}{3}\mu(p-3) \tag{1.2}$$

for the β-model. The intermittency coefficient μ plays the role of a correction to the $\zeta_p = p/3$ law, given by the K41 theory.

Even though all experimental results indicate the existence of a parameter like μ (Anselmet *et al.* 1984; Kerr 1985; Meneveau & Sreenivasan 1987*a*, 1991), the above theoretical models of intermittency have shown different inconsistencies when checking the numerical values of the power-law exponents ζ_p against the statistical analyses of the experimental and numerical data about of the velocity field (Anselmet *et al.* 1984; Kerr 1985; Vincent & Meneguzzi 1991). Inconsistencies have also been observed when fitting experimental measurements of the fractal distribution of the dissipative field by using the method of the Legendre transform (Frisch & Parisi 1985) for the multifractal model of turbulence (Meneveau & Sreenivasan 1987*a*, 1991).

Intermittency in turbulence can also be experimentally observed by directly determining the velocity PDFs which are generally characterized by a Gaussian shape at large scales (the energy-containing eddies) and become increasingly non-Gaussian at smaller scales. This last property is often interpreted as the effect of the self-stretching processes associated with the high-fluctuation vorticity structures (She 1991; She & Orzsag 1991). The fluctuations generated at small scales contribute to the experimentally observed tails of the PDFs and are often analytically approximated by exponential laws (She 1991; Benzi *et al.* 1991).

The statistical analysis of any turbulent flow is usually done by determining the high-order moments of the probability distribution functions. These are difficult to measure because of the poor statistics available near the extended tails of the probability distribution functions for any presently available set of experimental or numerical data. The fluctuations of the extended tails also cause large uncertainties when determining the ζ_p exponents of the velocity structure functions for large values of p. As a consequence, the measurement of the ζ_p exponents is usually done directly only for values of p below a given threshold p_{thres} while for larger values of p some authors have based their estimates on the extrapolation of the estimated PDFs (Anselmet *et al.* 1984; Meneveau & Sreenivasan 1991). The value of p_{thres} that selects the present direct reliable estimates is highly debated and is not likely to be $p_{thres} \geqslant 20$, at least for almost all available experimental (Anselmet *et al.* 1984; Meneveau & Sreenivasan 1991) and numerical (Kerr 1985; Vincent & Meneguzzi 1991; Metais & Lesieur 1992) data.

The present work reports a study of the large-scale statistical properties of three-dimensional homogeneous turbulence obtained by processing the data of a low-resolution (64^3) simulation which uses the simple Kraichnan eddy-viscosity model (Kraichnan 1976; Chollet & Lesieur 1981) for the parameterization of the small scales. The numerical experiment reproduces a self-similar range for energy, sub-

stantially comparable, in extent, with that obtained from direct numerical simulations performed with higher resolution as in the numerical experiment performed by Vincent & Meneguzzi (1991) (240^3 grid points) or by Kida & Ohkitani (1992) for highly symmetric flows.

The aim of this work is to show how the right statistics of the large-scale structures of a turbulent field can be reproduced in a low-resolution model using an eddy-viscosity parameterization like that of Kraichnan. This also allows one to exploit best the available degrees of freedom without the need of keeping track of the many degrees of freedom connected to the molecular viscosity. In the case of isotropic and stably stratified turbulence, a similar approach has been followed by Metais & Lesieur 1992.

This paper is composed of three sections. Section 1 describes the numerical method and the eddy-viscosity model. Section 2 discusses the statistical analysis of the velocity field on the basis of the PDFs. Section 3 compares our results on the values of the ζ_p power-law exponents to the known theories of intermittency as well as to the recent numerical and experimental measurements.

2. The numerical method and the eddy-viscosity model

The numerical simulation is performed by using a pseudo-spectral code with fully periodic boundary conditions. The numerical scheme is based on the explicit treatment of the dissipative term and is

$$\boldsymbol{u}_{\boldsymbol{k}}^{n+1} = \mathrm{e}^{-2\nu(k|k_c)k^2\Delta t}\,\boldsymbol{u}_{\boldsymbol{k}}^{n-1} + 2\,\Delta t\,\mathrm{e}^{-\nu(k|k_c)k^2\Delta t}\,\boldsymbol{H}_{\boldsymbol{k}}^{n}, \tag{2.1a}$$

$$\boldsymbol{H}_{\boldsymbol{k}} = \boldsymbol{H}'_{\boldsymbol{k}} - \frac{\boldsymbol{k}}{k^2}\left(\boldsymbol{k}\cdot\boldsymbol{H}'_{\boldsymbol{k}}\right), \tag{2.1b}$$

$$\boldsymbol{H}'_{\boldsymbol{k}} = (\boldsymbol{u}\times\boldsymbol{\omega})_{\boldsymbol{k}}, \tag{2.1c}$$

where $\boldsymbol{u}_{\boldsymbol{k}}$ is the Fourier component of the velocity vector field and $\nu(k|k_c)$ is the eddy-viscosity coefficient. In (2.1) the subscript $\boldsymbol{k}$ labels the Fourier components for wavenumbers $\boldsymbol{k} \subseteq [-N/2, +N/2]$, with $N = 64$, and the superscript n refers to time $t_n = n\Delta t$. The vector $\boldsymbol{\omega}$ is the vorticity field and $\boldsymbol{H}_{\boldsymbol{k}}$ is the nonlinear pseudo-spectral term: its computation requires nine three-dimensional FFTs to obtain the conservative formulation (Orszag 1971). Formula in (2.1*b*) removes the pressure and gives a divergence-free field. Forcing is obtained by keeping fixed the initial value of the Fourier components of the velocity field having wavenumbers modulus with $k \leqslant k_0$, with $k_0 = 1$.

A standard dealiasing technique (Orszag 1971) is used to remove the spurious components deriving from the pseudo-spectral computation of the nonlinear term. The technique exploits two shifted grids and spherical truncation for $k/k_{max} \geqslant (8/9)^{1/2}$. The integration scheme is the standard leap-frog with a second-order Euler predictor-corrector restart for stabilization each 50 time steps. The time step is $\Delta t = 0.01$ and the integration is performed for 10^4 time steps.

Small scales are parameterized by the Kraichnan's eddy-viscosity model (Kraichnan 1976; Chollet & Lesieur 1981)

$$\nu(k|k_c) = (a_1 + a_2\mathrm{e}^{-3.03k_c/k})\nu_e(k_c), \tag{2.2}$$

where $\nu_e(k_c) = (\tau_c k_c^2)^{-1} = (E(k_c)/k_c)^{1/2}$ is the viscosity based on the eddy turnover time $\tau_e = (E(k_c)k_c^3)^{-1/2}$ (Chollet & Lesieur 1981) corresponding to the numerical cut-off scale given by $k_c = (8/9)^{1/2}k_{max}$. The exponential term in (2.2) takes into account the contributions from the energy transfer around wavenumber k_c. The constants

a_1 and a_2 used in this numerical experiment are $a_1 = 0.15$ and $a_2 = 5$ and are in agreement with the results of other numerical simulations (Lesieur & Rogallo 1989) while theoretical results, in the framework of the Test-Field-Model theory of turbulence, give $a_1 = 0.267$ and $a_2 = 9$ (Chollet & Lesieur 1981). An analogous functional form of $v_e(k_c)$ is obtained in the more recent RNG theory of turbulence (Yakhot & Orszag 1986).

The initial conditions of the numerical simulation are a random realization of the energy spectrum

$$E(k) \approx \frac{k^4}{1 + (k/k_0)^{5/3+4}}, \tag{2.3}$$

with $k_0 = 1$. In particular, the Fourier velocity components are randomly generated from a three-dimensional symmetric Gaussian distribution having zero mean and variance in agreement with (2.3). The initial total energy is normalized to $E(t = 0) = 0.5$ and the characteristic velocity is $v_{rms} = (\frac{2}{3}E(t = 0))^{1/2} = 0.58$.

Supposing that the energy spectrum obeys over time Kolmogorov's law $E(k) = C_K \epsilon^{2/3} k^{-5/3}$ (where $C_K \approx 1.4$ is Kolmogorov's constant) within the range $[k_0\text{–}k_c]$, then the total energy involved in the cascade process is

$$E_t = \int_{k_0}^{\infty} E(k)\mathrm{d}k = C_K \epsilon^{2/3} \int_{k_0}^{\infty} k^{-5/3}\mathrm{d}k = \frac{3}{2} C_K \epsilon^{2/3} k_0^{-2/3}, \tag{2.4}$$

where the upper bound of the integral is assumed to be ∞ for sufficiently large values of k_c; the corresponding energy dissipation rate ϵ is

$$\epsilon = C_K^{-3/2} v_{rms}^3 k_0. \tag{2.5}$$

Using (2.5), the energy spectrum $E(k)$ then becomes

$$E(k) = v_{rms}^2 k_0^{2/3} k^{-5/3}. \tag{2.6}$$

Formula (2.6), calculated at k_c, allows one to obtain the coefficient $v_e(k_c) = v_{rms}(k_0/k_c^4)^{1/3}$ as an explicit function of the r.m.s. velocity and the wavenumber cutoff k_c. In practice, the eddy viscosity $v_e(k_c)$ is computed each 50 time steps, when restarting the leap-frog scheme (Briscolini & Santangelo 1992).

Some physical parameters of the simulation can be estimated by using formula (2.6) for the energy spectrum. They are the total enstrophy

$$\Omega(t) \approx \int_{k_0}^{k_c} k^2 E(k)\mathrm{d}k = \tfrac{3}{4} v_{rms}^2 k_0^{2/3} k_c^{4/3} \approx 25, \tag{2.7}$$

the *effective* Taylor dissipation length

$$\lambda(t) = [E(t)/\Omega(t)]^{1/2} \approx 2^{1/2}(k_0 k_c^2)^{-1/3} \approx 0.15, \tag{2.8}$$

and the *effective* Taylor microscale Reynolds number

$$Re_\lambda = v_{rms}\lambda/v_{eff} \approx (2C_K)^{1/2}\gamma^{-4/3}(k_c/k_0)^{2/3} \approx 138, \tag{2.9}$$

where

$$v_{eff} = \epsilon^{1/3}\left(\frac{\gamma}{k_c}\right)^{4/3} \approx C_K^{-1/2} v_{rms} k_0^{1/3}\left(\frac{\gamma}{k_c}\right)^{4/3} \approx 6 \times 10^{-4} \tag{2.10}$$

is the *effective* viscosity coefficient with $\gamma \approx 0.2$ (Yakhot & Orszag 1986). The *effective* attribute used in these formulae underlines the use of a large-eddy *subgrid-scale* dissipation model in place of an ordinary molecular viscosity, where terms like

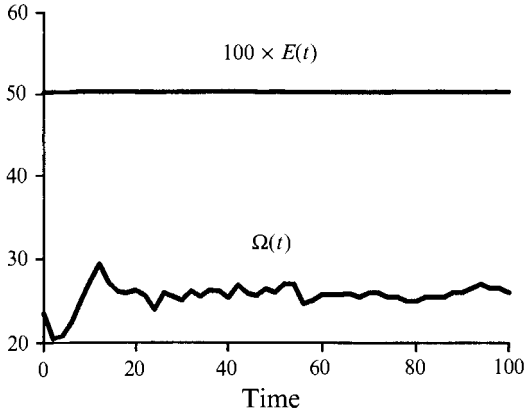

FIGURE 1. The temporal evolution of total energy and total enstrophy. Note how forcing conserves remarkably the initial value of the energy, which shows only weak fluctuations (less than 1%). The enstrophy shows larger fluctuations, of the order of 10%, except during the initial transient phase. Note also how the value of the enstrophy $\Omega \approx 25$ is in agreement with the value estimated in (2.7).

viscosity or Taylor-microscale Reynolds number have a direct meaning. Comparing (2.10) with (2.2), the constant $a_1 = \gamma^{4/3} C_K^{-1/2} \approx 0.1$ has a value close to that used in our numerical experiment. Then, the most significant timescales are the macroscale eddy turnover time

$$\tau_0 = (v_{rms} k_0)^{-1} \approx 1.7, \tag{2.11}$$

and the *effective* microscale eddy turnover time

$$\tau_c = (v_{rms} k_c)^{-1} \approx 0.06. \tag{2.12}$$

The formula for τ_c allows one to estimate the time step of the numerical integration which appears in good agreement with the value actually used, $\Delta t = 10^{-2}$.

The temporal evolution of the total energy $E(t)$ and of the total enstrophy $\Omega(t)$ are reported in figure 1. The behaviour of the energy shows weak fluctuations (less than 1%), reflecting a balance between forcing at large scales and dissipation at small scales. Similarly, after an initial transient phase, the time evolution of the enstrophy shows only moderately larger fluctuations, at the level of 10%. The transient shows an initial decaying phase followed by a successive increase of the enstrophy due to nonlinear vortex-stretching mechanisms. Other authors (see e.g. Kerr 1985; Vincent & Meneguzzi 1991) find larger energy fluctuations with time because of the use of different forcing methods at low wavenumbers.

Figure 2(*a*) shows the log-log plot of the energy spectrum at the end of the simulation. No intermediate energy spectra are shown because, during the evolution, the spectrum is stationary and does not change significantly. A self-similar energy-scaling range extends over all available numerical scales from k_0 to k_c. It may also be noted that there is no appreciable numerical noise at small scales, where the exponential cutoff efficiently dissipates the energy. It is remarkable that the self-similar range is as extended as in numerical experiments performed with much higher numerical resolution like those by Vincent & Meneguzzi (1991) or by Kida & Ohkitani (1992) which report similar values for the physical parameters like the *effective* Taylor-microscale Reynolds number Re_λ and the *effective* viscosity coeffi-

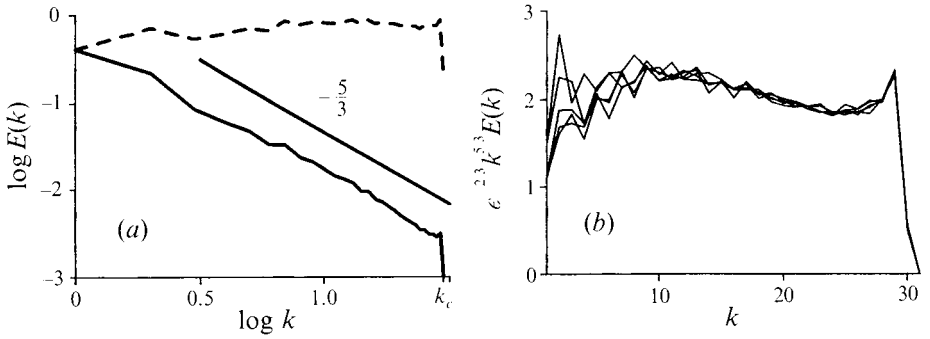

FIGURE 2. (*a*) The final energy spectrum after 10^4 time steps. The dashed line represents the curve $E(k)k^{5/3}$. The inertial range appears correctly reproduced for most numerical scales, from $k_0 = 1$, where forcing is applied, to the rightmost boundary k_c, corresponding to the exponential cutoff of the eddy-viscosity model. (*b*) Linear plot of the compensated spectra $\epsilon^{-2/3}k^{5/3}E(k)$ versus the wavenumber k for configurations 5, 10, 15, 20, and 25 of our sample of 25 statistically independent configurations. The use of linear axes allows a rather accurate estimate of the behaviour of the dissipation ϵ which does not deviate more than 20% from its mean value. Note how this result does not contradict the contents of (*a*) where the log-log plot shows a large extent of the inertial range. This figure also allows one to estimate directly the value of the Kolmogorov's constant $C_K \sim 2$.

cient ν_{eff}. The similarity of the physical parameters and the analogous extent of the self-similar energy spectrum indicate that the simulations can be compared efficaciously.

A more detailed estimate of the reliability of the wide extent of the inertial range, shown figure 2(*a*), can only be obtained from a more quantitative analysis of the dependence of the dissipation versus the wavenumbers. To this end, we have reported in figure 2(*b*) the compensated spectra $\epsilon^{-2/3}k^{5/3}E(k)$ versus the wavenumbers. The use of linear rather than logarithmic axes allows one to estimate how dissipation shows deviations of the order of 20% across the different scales and allows a comparison with other published results (see e.g. Metais & Lesieur 1992 and references therein). It is also important to stress that, while these fluctuations are clearly apparent when using the linear plot, there is little if any contradiction with our above statement about the extent of the inertial range which is naturally appreciated using the proper log-log plot of figure 2(*a*). Figure 2(*b*) can also be used to estimate directly the value of Kolmogorov's constant C_K which we have found to be in reasonable agreement with the results found by other authors (see e.g. Monin & Yaglom 1975; Vincent & Meneguzzi 1991; Metais & Lesieur 1992).

An example of the space configuration of the vorticity field is reported in figures 3 and 4 by showing the vorticity structures that satisfy the criterion $(\omega^2 - \langle\omega^2\rangle)/(\langle\omega^4 - \langle\omega^2\rangle^2\rangle^{1/2}) \geqslant f_{th}$, for $f_{th} = 2$ and 4 respectively, where the $\langle\rangle$ symbol is the simple space average. For large values of f_{th}, this criterion identifies the regions of the computational domain where vorticity fluctuations are significant and the related intermittent phenomena are expected to take place. Some structures appear strongly elongated and randomly oriented in space. Their characteristic length is of the order of a third of the entire computational domain, in rough agreement with the properties of the structures observed by Vincent & Meneguzzi (1991) in their figure 13. The effect of the lower numerical resolution clearly appears when comparing the two figures. At low resolution a smaller number of vorticity structures are

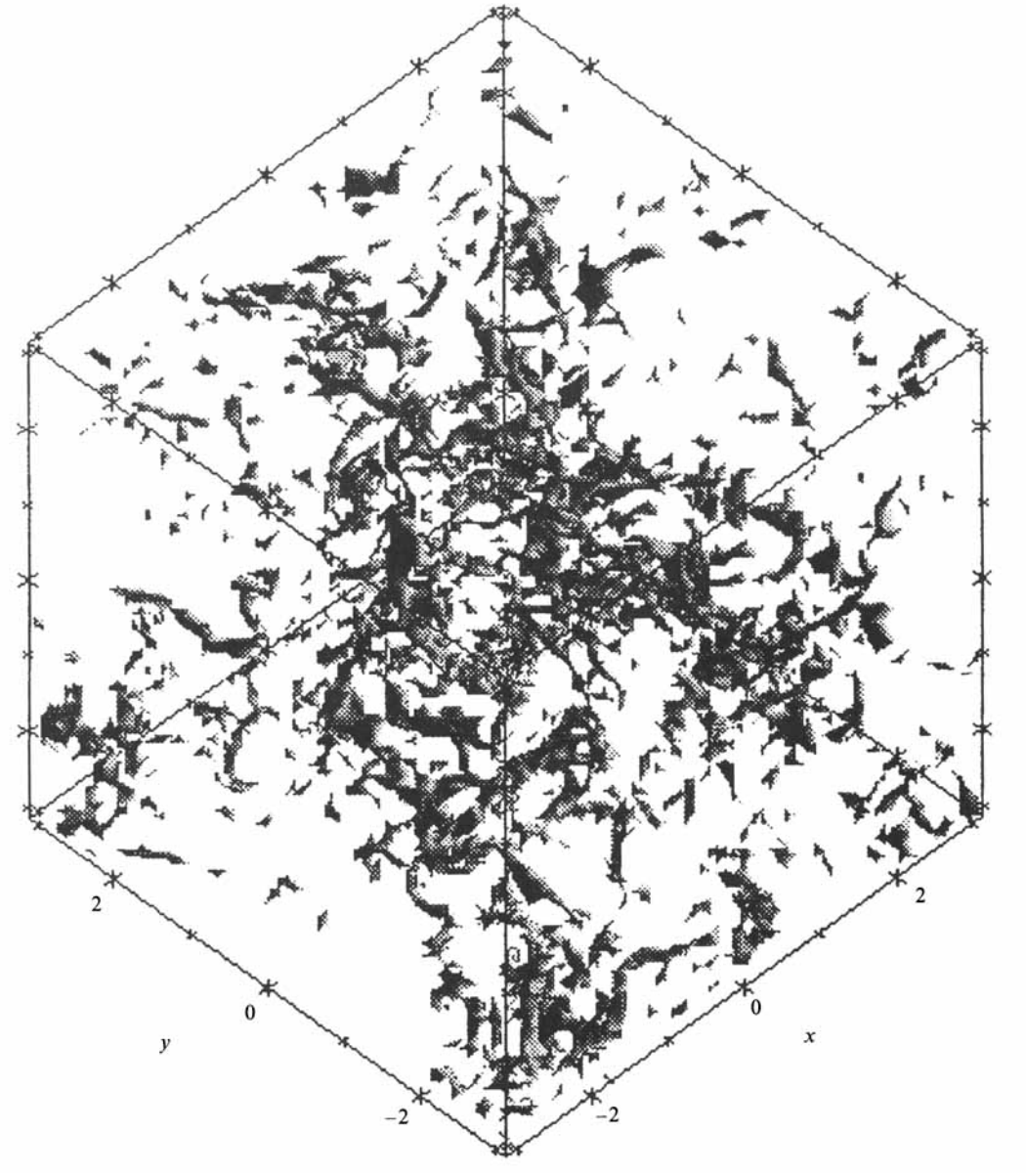

FIGURE 3. An example of the spatial configuration of the vorticity field. The figure shows the regions of space where $(\omega^2 - \langle\omega^2\rangle)/(\langle\omega^4 - \langle\omega^2\rangle^2\rangle^{1/2}) \geqslant f_{th}$ for $f_{th} = 2$. The criterion selects the regions of space where vorticity fluctuations are particularly strong and indicates the corresponding space distribution of the intermittent dynamics. Some thin and elongated vorticity structures are easily observable and extend approximately for $20\Delta x$.

apparent but they are only moderately thicker than those observed with the high-resolution direct simulations. Notwithstanding these minor differences, the eddy-viscosity parameterization of turbulence appears to reproduce reasonably well the large-scale structures of the vorticity field within the dynamical scales that belong to the self-similar range.

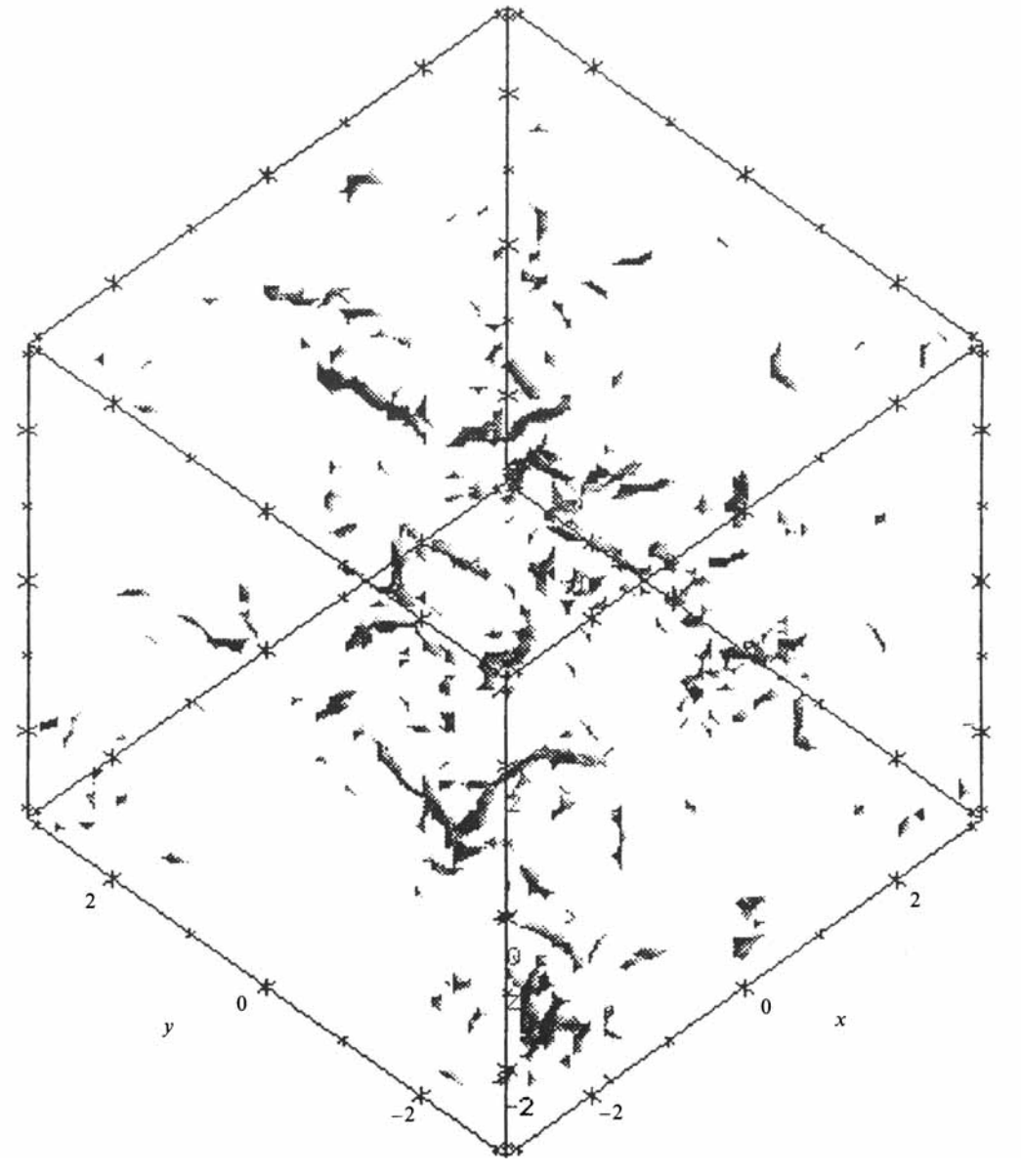

FIGURE 4. The same as in figure 3 but for $f_{th} = 4$. A smaller number of thinner vorticity structures are shown. The larger value of the threshold used here selects more clearly the coherent vortical structure of the flow.

3. Probability distribution function of the velocity field

The statistical analysis of three-dimensional turbulence is performed by estimating the probability distributions and the correlation functions of the velocity field. A detailed and reliable statistical analysis obviously requires the treatment of a large number of successive and independent velocity configurations, and an accepted criterion that ensures the required statistical independence, is that the time interval between successive configurations be comparable with the macroscale eddy turnover time. For the present simulation, the value of $\tau_0 \approx 1.7$ (see (2.11)) suggests the

recording of a velocity configuration each 400 time steps, which corresponds to a couple of macroscale eddy turnover times. Since the simulation spans 10^4 time steps, an ensemble of 25 statistically independent velocity configurations can be obtained for a total amount of $25 \times 64^3 \approx 7 \times 10^6$ samples. In the present study, the recording of many different configurations is also useful for balancing the use of low resolution.

In order to define more accurately the actual number of independent space samples of a given configuration, the Taylor dissipation length λ of (2.8) can be used instead of the mesh size Δx. In this simulation, which is based on the use of Kraichnan's eddy-viscosity model, this is not a major correction to the previous approximate estimate so that the total number of independent samples only reduces moderately to $25 \times 64^3 \times (\lambda/\Delta x)^{-3} \sim 2 \times 10^6$.

An important statistical measure of intermittency is given by the structure functions $F_p(r) = \langle |\delta u_x(r)|^p \rangle$ which are defined as the pth moments of the velocity differences $\delta u_x(r) = u_x(\boldsymbol{x} + \boldsymbol{r}) - u_x(\boldsymbol{x})$, which depend only on r for homogeneous isotropic turbulence. The evaluation of the velocity differences from the numerical data requires an average over all pairs of grid points which are separated by distance r. This is a long numerical process that we have shortened by including in the average only those pairs of points which are aligned along the three orthogonal directions of space x, y and z. This reduced procedure decreases the statistics but guarantees that both the longitudinal as well as the two transverse velocity components are included in the averaging process.

Figure 5(*a*) shows the probability distribution function of the dimensionless variable

$$\xi(r) = \delta u_x(r) / \langle \delta u_x(r)^2 \rangle^{1/2} \tag{3.1}$$

for some values of r. The corresponding histogram is obtained by grouping the available data in 64 bins of width $\Delta\xi \approx 0.47$, corresponding to a range of 15 standard deviations. The adopted binning parameters are a good compromise in order to measure reliably the extent and the shape of the tails of the distribution function. The data of the 25 statistically independent configurations are averaged to produce the two probability distribution functions shown in figure 5(*a*), where they are compared with the Gaussian distribution and with the data reported by Vincent & Meneguzzi 1991. It appears that the main features of the PDFs obtained from the high-resolution direct numerical simulation are reproduced. These features are: (i) the increase of the non-Gaussian nature of the PDFs with the decrease of the space scale r used to compute the distribution; and (ii) the development of clear exponential tails for small space scales. It is now possible to understand how some of the small-scale spatial patterns shown in figures 3 and 4, that correspond to large fluctuations of the vorticity, are the very probable cause of the extended non-Gaussian tails of the PDFs.

It is not easy to find a *simple* analytical approximation to the velocity PDFs (like those shown in figure 5*a*) which is valid over the full range of definition of ξ. Even though analytical approximations have been attempted by some authors (Castaigne *et al.* 1990; Kraichnan 1990; Meneveau & Sreenivasan 1991; She & Orzsag 1991; Benzi *et al.* 1991), we prefer to perform a *piece-wise* or *local* interpolation to the PDFs, of figure 5(*a*), by means of the simpler formula $P(\xi) \sim \mathrm{e}^{-\beta|\xi|^\alpha}$, where α and β are parameters that depend on ξ, and the result is shown in figure 5(*b*). Using the PDF at $r = 9\Delta x$, the asymptotic value of $\alpha \approx 1.7$ (dot-dashed line) is in agreement with the value of α estimated in figure 8 on the basis of the positions of the maxima of the PDFs of the moments. For smaller scales, the PDFs show an

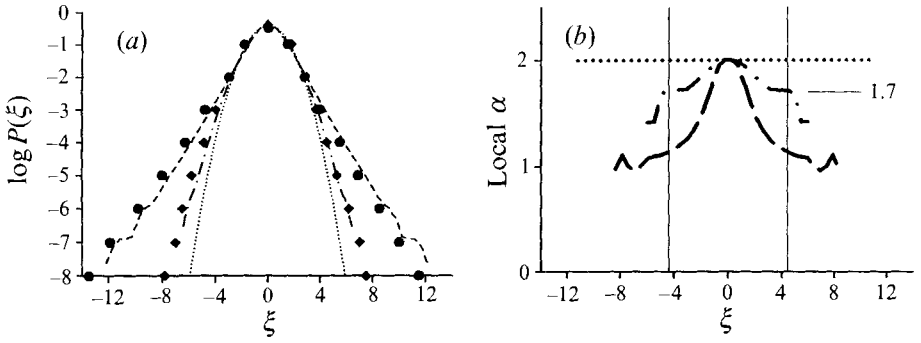

FIGURE 5. (*a*) Log-linear plot of the probability distribution functions (PDFs) $P(\xi(r))$ for the normalized velocity $\xi(r) = \delta u(r)/\langle \delta u(r)^2 \rangle^{1/2}$ for two different scales $r = \Delta x \approx 0.1$ (— — —) and $r = 9\Delta x \approx 0.9$ (— · —), compared with the Gaussian distribution (· · ·) and with the data from the high-resolution numerical experiment by Vincent and Meneguzzi (1991) (• • • and ◆◆◆ represent the data of their experiment for the dissipative and the inertial range respectively). The number of bins of each histogram is 64 for a maximum amount of 15 standard deviations and $\Delta\xi \approx 0.47$. (*b*) Plot of the *local* value of α *vs.* the variable $\xi(r)$, defined in (*a*), assuming a *piece-wise* representation of $P(\xi) \sim e^{-\beta|\xi|^\alpha}$. The curves are as in (*a*), and the reference horizontal line $\alpha = -2$, corresponding to the simple Gaussian distribution, is shown for comparison. This plot shows clearly how the probability distribution function deviates more and more from Gaussianity and tends to an exponential distribution for small values of r and for large deviations from the mean. The maximum deviations from Gaussianity decrease with larger values of r, where exponential tails are never obtained. In particular, for $r = 9\Delta x$, the limiting α, at large deviations, is 1.7, in agreement with the results of figure 8 where the value of α is directly measured from the slope of the position of the maxima of the moments of the PDFs. The vertical confidence bars are drawn at $\pm 5\xi$, as in figure 7, where they limit the largest maximum deviation for which the maxima of the moments of the PDFs can be measured reliably. Note how errors dominate the estimate of α, consistently with the same limiting threshold reported in figure 7.

increasing asymptotic exponential behaviour, as indicated by the limiting case of the PDF for $r = \Delta x$ (long dashed line).

Other authors (see e.g. Kida & Murakami 1989; Kraichnan 1990; Benzi *et al.* 1991) prefer different approximations to the PDFs based on the more complex formula $P(\xi) \sim \xi^\gamma e^{-\beta|\xi|^\alpha}$, which is expected to fit better the experimental and numerical data. We use two ways to estimate the value of γ: the direct nonlinear fit of the PDFs and a reinterpretation of figure 8. The former has indicated non-negligible values of $\gamma \sim -0.5$ only for the small-scale PDFs. The latter, based on the usage of the quantity $\log(p+\gamma)$ instead of $\log(p)$ on the horizontal axis of figure 8 (Kida & Murakami 1989), indicates negligible value of γ, which is not surprising, since the reported data derive from the PDFs which are characteristic of the inertial range.

Besides this basic agreement regarding the non-Gaussian statistics, other parameters like the *skewness* S and the *flatness* F of the PDFs of the velocity gradients give further confidence in the validity of the model. The PDFs for two variables $\partial_y u_x$ and $\partial_z u_x$ give consistent values of the *flatness* $F \sim 4.5$ and are thus in agreement with other numerical experiments (Kerr 1985; Metais & Lesieur 1992); the distribution functions are also highly symmetric and the corresponding values of the *skewness* are small ($S \approx 0.06$) and are comparable with those reported by Vincent & Meneguzzi 1991. The *skewness* of the longitudinal velocity gradient $\partial_x u_x$ is $S \approx -0.35$, a value which is clearly less than the value $S = -0.5$, asymptotically approximated in the case of homogeneous flows at $Re_\lambda > 20$ (see Kerr 1985) and theoretically predicted in

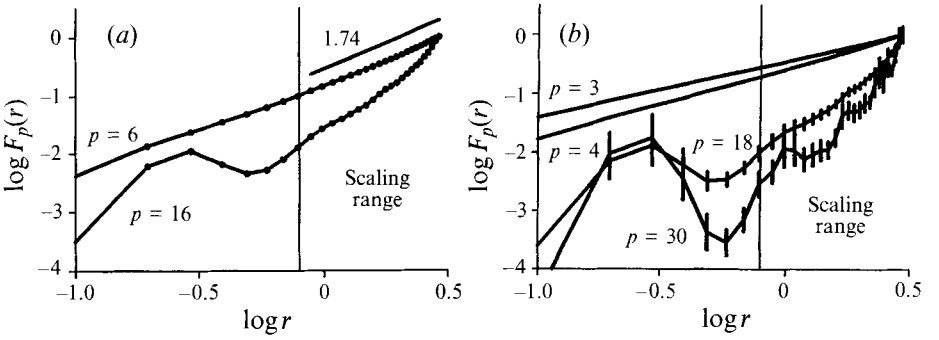

FIGURE 6. (*a*) The log-log plot of the structure function $F_p(r) = \langle |\delta u(r)|^p \rangle$ versus r for $p = 6$ and 16. The dots mark the values of r where data is available. The *scaling range* spans from $9\Delta x$ to $32\Delta x$. The curves are fitted by means of the least-squares linear fit to get the ζ_p slope. The intermittency coefficient is $\mu = 2 - \zeta_6 = 0.26$. Moments computed at small scales are strongly affected by fluctuations which increase with the order of the moments. (*b*) The same as in (*a*) but for $p = 3, 4, 18$, and 30. The error bars are the *r.m.s.* of the moments obtained from the 25 statistically independent configurations. The corresponding errors for $p = 3$ and 4 are negligible and are not shown.

Yakhot & Orszag 1986. This discrepancy can be interpreted as an effect of the low numerical resolution which affects the computation of S (see e.g. Antonia *et al.* 1982), where an analysis of the dependency of S on time sampling is reported) and reflects the existence of the exponential cutoff due to the eddy-viscosity approximation of the nonlinear transfer near the dissipation wavenumber k_c. In fact, near k_c, the kinetic energy of the flow is strongly damped, thus inhibiting the stretching of thin vortices that are instead dissipated rapidly when their thickness is of the order of a few grid points.

An important measure of spatial intermittency is given by the *intermittency coefficient* μ which is defined by the spatial correlation of the dissipation rate $\langle \epsilon(x)\epsilon(x+r) \rangle \sim r^{-\mu}$. A possible alternative way to measure the coefficient μ is given by means of the sixth-order moments of the velocity PDFs. In fact, using the assumption that $\epsilon \sim \delta v^3 / r$ (Monin & Yaglom 1975) one obtains $\langle \epsilon(x)\epsilon(x+r) \rangle \sim \langle \delta v(r)^6 \rangle / r^2 \sim r^{\zeta_6 - 2}$ and $\mu = \zeta_6 - 2$. (See Anselmet *et al.* 1984 and, more recently, Sreenivasan & Kailasnath 1993 for a discussion on the dependence of the value of the μ parameter on the different ways of processing of the experimental data.) Here we have decided to measure the intermittency coefficient μ by means of the sixth-order structure functions and the plot of $\langle \delta v(r)^6 \rangle$ versus r is reported in a log-log form in figure 6(*a*) where the ζ_6 exponent can be obtained from the slope of the curve that best fits the data. The right estimate of the slope of the curve depends on the fitting interval which should be confined to the inertial range of the energy cascade which is bound, at small scales, by the dissipative range. The extent of the latter depends on the dissipation model used and, in our simulation, which is based on Kraichnan's eddy viscosity, dissipation appears to affect only a tiny range of small space scales. This is clearly seen from the energy spectrum (figure 2*a*) and from the sixth-order structure functions (figure 6*a*) which both exhibit a clean power-law shape on all available space scales, except the smallest ones.

The least-squares fit applied to the whole scaling range, shown in figure 6(*a*) for $p = 6$, after the removal of the first two smallest scales, gives an intermittency coefficient $\mu \approx 0.35$ which compares reasonably with previous estimates based on ex-

perimental and numerical data (Anselmet *et al.* 1984; Meneveau & Sreenivasan 1991; Vincent & Meneguzzi 1991). There is general agreement that the exact measurement of μ is a difficult task and that the measurements obtained from the moment of order 6 lead to an overestimate of its value (Antonia *et al.* 1982; Anselmet *et al.* 1984). Commonly μ is considered closer to 0.20 as a consequence of its direct measurement which is based the scaling properties of the correlation function of the energy dissipation (Kolmogorov 1962; Kraichnan 1974; Anselmet *et al.* 1984).

Figures 6(*a*) and 6(*b*) show how the structure functions corresponding to increasing values of the moments p exhibit a narrower extent of the *scaling range*. In order to fit the slopes of these higher-order structure functions we remark that figures 6(*a*) and 6(*b*) suggest that the interval, bound at the left by $r = 9\Delta x$, identifies a reasonable self-similar *scaling range*. The re-estimate of the intermittency coefficient on the basis of this range of scales gives a somewhat different value of $\mu = 0.26$ which is in closer agreement with the recent measurements reported by Sreenivasan & Kailasnath 1993. Figure 6(*b*) shows the structure functions for other values of the moment, $p = 3$, 4, 18 and 30, together with the errors of the mean values. The errors have been simply obtained from the r.m.s. of the sampled data and are negligible for $p = 3$ and 4. For large values of the moments the errors are not very large but help to give further confidence in the extent of the *scaling range*.

4. High-order statistics

The main difficulty of an accurate estimate of the high-order moments of any probability distribution function $P(\xi)$, obtained from experimental data, is due to the finite number of available samples of the random variable. In fact, high-order moments depend on the positions of the maxima of the functions $\xi^p P(\xi)$ for large values of p. For simple and bell-shaped functions, the maxima of $\xi^p P(\xi)$, say $\xi_{max}(p)$, are located several standard deviations from the centre of the base distribution function $P(\xi)$, where the statistics is always poor, for any available number of sampled data. This effect is clearly observable in figure 7 where $\xi^p P(\xi)$ is reported versus ξ for $r = 9\Delta x$ and different values of p. The plot shows that, for $p > 16$, the positions of maxima cannot be distinguished or are subject to large uncertainties.

On this basis, a simple argument can be used for estimating *a priori* the index of the highest available moment obtainable from a limited amount of data. The argument is based on the assumption that a reasonable analytic approximation of the probability distribution function is $P(\xi) \sim \mathrm{e}^{-\beta|\xi|^\alpha}$ (Castaigne *et al.* 1990; Meneveau & Sreenivasan 1991; She 1991; Benzi *et al.* 1991) where the exponent α assumes values ranging from 2.0 (Gaussian distribution) to 1.0 (exponential distribution). The position of the maximum of $\xi^p P(\xi)$ is then

$$\xi_{max}(p) = \left(\frac{p}{\beta\alpha}\right)^{1/\alpha}. \tag{4.1}$$

A reasonable estimate of the position of the maximum in the histogram of $\xi^p P(\xi)$ requires that at least $N_b \approx 10^2$ samples be found in the bin corresponding to the maximum, so that the statistical uncertainty ($N_b^{-1/2} \approx 0.1$) be at most 10%. This condition requires $N_{tot} P(\xi_{max}(p)) \Delta\xi \geqslant 100$ where $\Delta\xi$ is the width of a bin of the histogram. Using (4.1) the previous constraint gives

$$p \leqslant \alpha \log_e (0.01\, N_{tot}\, \Delta\xi). \tag{4.2}$$

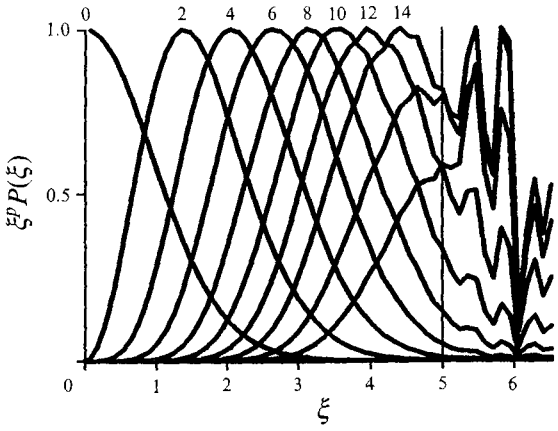

FIGURE 7. Probability distribution functions of the moments of the normalized velocity difference $\xi(r) = \delta u(r)/\langle \delta u(r)^2 \rangle^{1/2}$ at scale $r = 9\Delta x$. The different curves correspond to the moments up to order 18 and are shown scaled to the same maximum value. The vertical bar clearly identifies the maximum value of p for which the statistics is sufficient to allow a reliable measurement of the parameters of the PDF. It is apparent that the value of ζ_p can be safely determined only for $p \leqslant 16$.

Figure 8 shows the positions of the maxima of the histograms of $\xi^p P(\xi)$ versus p in a log-log plot for values of r near the lower bound of the *scaling range* ($r = 9\Delta x \approx 0.9$). The range of p is from 2 to 16 and the data are well fitted by a straight line $\log(\xi_{max}(p)) = 0.6 \log(p) + constant$ and the corresponding slope $\alpha = 1/0.6 \approx 1.7$, a value which is in agreement with the asymptotic local value of the α exponent shown in figure 5(*b*). For the present simulation, where 25 statistically independent configurations are available with a total number of 10^7 samples, and $\Delta\xi \approx 0.47$, p must be less than 18, a value comparable with that obtained by a qualitative analysis of figure 7. For a single configuration only $10^7/25$ samples are available and the corresponding maximum value of the ζ_p exponents that can be measured reliably is ~ 12. It is interesting to observe that, according to (4.2), and with the amount of data available to Vincent & Meneguzzi 1991 in their numerical experiment (of the order of 10^9) they should have been able to measure the ζ_p moments up to $p = 26$, which is in approximate agreement with their claim.

A correct use of the (4.2) requires that the estimate of the total number of independent samples N_{tot} be based on the assumption of spatial and temporal statistical independence of the hydrodynamic signal. The above estimate of $N_{tot} \sim 10^7$ is based on the grid size and is an overestimate because of the obvious dissipative correlations at small scales. A more reliable estimate can be based on the Taylor dissipation length $\lambda \sim 0.15$ of (2.8). Using this latter, the above reliability estimates for the moments should be decreased by the quantity $\Delta p = -\alpha \log_e[(\lambda/\Delta x)^3] \sim 2.2$, a result which makes our estimates in even greater agreement with the contents of figure 7. Correspondingly, when using molecular viscosity, where the dissipative range extends over a much broader range of wavenumbers, the above-mentioned Δp correction to the ζ_p exponents might be substantially larger because the value of the Taylor dissipation length is much larger than the grid size Δx.

Another correction to the estimate of the reliability of the moments comes from the assumption about the analytical expression of the probability distribution function of $P(\xi)$. If we use the function $P(\xi) \sim \xi^\gamma e^{-\beta|\xi|^\alpha}$ (Kida & Murakami 1989; Kraichnan 1990; Benzi *et al.* 1991; Metais & Lesieur 1992), the reliability estimates

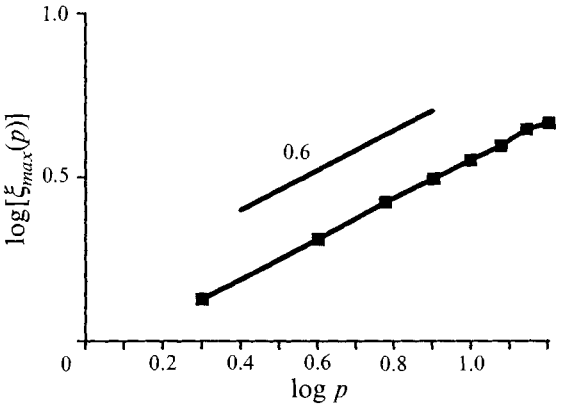

FIGURE 8. The log-log plot of the positions of the maxima of the PDFs of the moments of the normalized velocity difference $\xi(r) = \delta u(r)/\langle \delta u(r)^2 \rangle^{1/2}$ versus p, at scale $r = 9\Delta x \approx 0.9$. The slope gives the value of $\alpha = 1/0.6 \approx 1.7$, in agreement with the results shown in figure 5(*b*). This is a measure of the exponent α of the velocity PDF according to the formula $P(\xi) \sim e^{-\beta|\xi|^\alpha}$.

of p are shifted by γ, but only slightly, since our previous estimates of γ are negligible in the inertial range. In any case, the other published results for γ do not exceed unity and those do not alter significantly our conclusions.

The ζ_p exponents are numerically estimated on the basis that the pth-order structure functions $\langle |\delta u_x(r)|^p \rangle$ versus r scale as power laws $\sim r^{\zeta_p}$. In a log-log plot, the ζ_p exponents can be estimated by using the weighted least-squares method (Press *et al.* 1989). All our fits have been applied to the *scaling range* ($9\Delta x \leqslant r \leqslant 32\Delta x$) identified in figures 6(*a*) and 6(*b*) where the structure function data show an approximate linear behaviour for values of p in the range $p \leqslant 16$.

The availability of 25 statistically independent sets of structure functions, corresponding to the 25 field configurations, poses the problem of the right averaging process that best exploits the available data. We have found that there is no unique and optimal way to average the available data for a given pth-order structure function. The simplest way is obviously the straightforward least-square fit applied to the *mean* pth-order structure function, as they are obtained by calculating the mean values, and the related r.m.s. deviations, from the raw data corresponding to the 25 independent configurations.

The final result is reported in figure 9 where the ζ_p exponents are estimated with *unweighted* least-squares linear fits and are reported versus p. The plot is divided in two parts: the left side corresponds to the ζ_p exponents with order p less than or equal to 16, which can be measured more accurately (on the basis of (4.2) and of the results shown in figure 7), while the right part corresponds to the more uncertain moments of higher order where the statistics is poorer. Notwithstanding the reduced accuracy of the ζ_p exponents for large values of p, figure 9(*a*) shows that our data are in good agreement with the results obtained in the high-resolution numerical experiment of Vincent & Meneguzzi (1991). Some minor deviations between our data and their results may depend on the different values of ζ_2, which is here assumed to be 0.67, as in the K41 theory, while it is close to 0.69 in their paper. The same reasoning applies to the data of Anselmet *et al.* (1984) where $\zeta_2 = 0.71$. This argument has been validated by plotting the *dimensionless structure functions* $\theta_p = \zeta_p - p/3\zeta_2$ (not shown) and no major disagreement has been found.

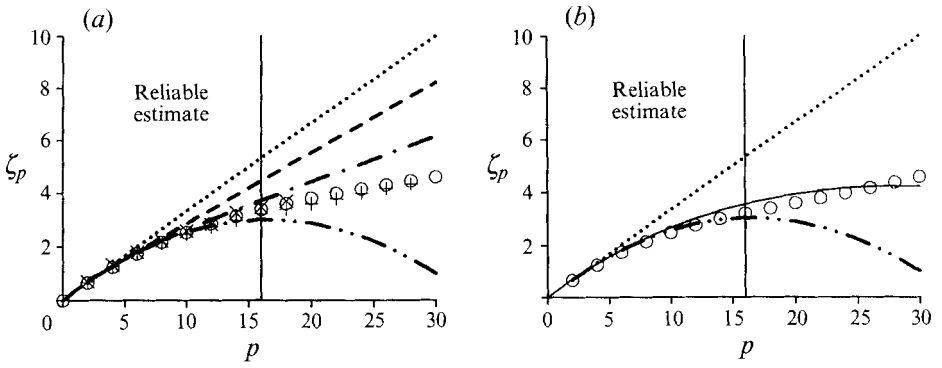

FIGURE 9. The plot of the ζ_p exponents of the structure functions versus p for the simulation of this paper (o o o) compared with data from the K41 theory (Kolmogorov 1941) (· · ·), the log-normal distribution (Monin & Yaglom 1975) (—··—), the β-model (Frisch *et al.* 1978) (— — —), the p-model with $p = 0.7$ (Meneveau & Sreenivasan 1987*b*) (—·—), the data of the numerical experiment of Vincent & Meneguzzi (1991) (+ + +) and the experimental measurements of Anselmet *et al.* (1984) (× × ×). The vertical bar identifies the left part of the plot, where the statistics of the numerical simulation reported in this paper is sufficient to estimate reliably the ζ_p exponents. In (*b*), the thin continuous line represents the log-stable distribution model (see Kida 1991) with parameters $\mu = 0.2$ and $\alpha = 1.66$.

Besides the basic agreement among the different experimental and numerical results shown in figure 9 it is also necessary to indicate the reliability and the errors related to the estimates of the ζ_p exponents which, in turn, depend on the errors of the estimate of the slope of the pth-order structure functions versus r. The first attempt to get an indication about these errors has been done using the *weighted* least-squares method where the weights are the standard deviations of the values of the pth-order structure functions for the different scales r. The results of the statistical analysis give almost negligible errors for the estimate of the ζ_p exponents for $p < 16$, which increase only at the 10% level for $p \sim 25$–30.

An unpleasant result is given by the values of the χ^2 reliability test of the *weighted* least-squares linear fits which show unreasonably small values, even for small values of p, which is in clear disagreement with the evidence that the *scaling range* is clearly identified, at least for $p \leqslant 10$. We interpret this phenomenon as a consequence of an overestimate of the errors associated with the data points used for the fits. We have investigated directly this conjecture, by plotting versus r the pth-order structure functions for each temporal configuration, and we have observed that the data, corresponding to the different configurations, all show an approximately consistent linear behaviour but with large vertical shifts and only smaller fluctuations of the slope. This clearly indicates that the corresponding r.m.s. deviations of the mean values must be large as a consequence of the fact that an uncorrelated systematic component is probably contributing to the total r.m.s. deviations according to the formula $\sigma_p^2(r)_{total} = \sigma_p^2(r) + \sigma_p^2(r)_{systematic}$. The physical origin of this systematic component is not clear and is probably due to the influence and to the varying number of coherent structures of the flow that obviously changes in space and in time among configurations. In other words the probable physical origin of the systematic component is the temporal intermittency of flow which is hard to include in any analysis which is only based on spatial intermittency. We will return to this important argument in more detail when discussing figure 11.

Assuming that a systematic component is afflicting our statistical analysis we make an attempt to reduce its influence on the final result by 'compressing' the pth-order structure functions corresponding to the different configurations. Since there is no unique way to obtain this result we have decided to adopt the simple strategy of imposing that the structure functions, for a given p, all pass through a unique point at scale $r = 15\Delta x$. This procedure resulted in more reliable estimates of the parameters obtained from the *weighted* least-squares fits, as we have observed from the values of the χ^2 variable, that now do not show the uncomfortably small values obtained without this type of treatment of the data.

Figures 10(*a*) and 10(*b*) show the behaviour of the ζ_p exponents versus p when using the *unweighted* and *weighted* least-squares linear fit methods respectively. The main conclusions that can be drawn from the figures are that: (i) the results are in agreement with those obtained in figure 9 inside the *reliable* range (thus confirming a reasonable agreement with other experimental and numerical data), (ii) they deviate significantly from the results of figure 9 only outside the *reliable* range (corresponding to an apparently less intermittent behaviour), and (iii) that the $\pm 1\sigma$ confidence bounds indicate a small (less than 30%) measurement error even for large values of p. Points (ii) and (iii) are only apparently inconsistent because they pertain to the *unreliable* range that we have estimated on the basis of a clear and independent statistical argument such as that given by (4.2) and shown qualitatively in figure 7. Also, following the same line of reasoning, figure 7 shows how the apparent precision of the measurements of the ζ_p exponents should not be a suprise, simply because these measurements reflect a precise determination of a wrong quantity. In fact, for large values of p, the maxima of the probability distribution of the moments are statistically bound by the constraint of (4.2), which is located well before the maxima could be achieved with a limited amount of data. In other words, for large values of p, the measurement of the ζ_p exponents simply determine 'precisely' the bound indicated by (4.2) which has no physical meaning but rather reflects how our statistics is not able to determine the ζ_p exponents for large values of p.

We have investigated in more detail the origin of the large systematic fluctuations of the values of the structure functions that we have discussed above and we have concluded that these are strongly connected to the *temporal intermittency* of the system. To this end, we have plotted in detail the ζ_p exponents versus p for each configuration and we have reported the results in figure 11. The inspection of the results shows that the single curves are not affected by any noise, which can be due to the poorer available statistics, but rather, even inside the *reliable* range, the curves can be naturally grouped into at least two classes: (i) in figure 11(*a*), the set of configurations that show a behaviour similar to the *mean* results shown in figures 9 and 10, and (ii) in figure 11(*b*), a smaller set of configurations that show a much stronger intermittency with curves that exhibit a behaviour which loosely resembles the Kolmogorov–Obukhov log-normal model (Kolmogorov 1962; Obukhov 1962; Monin & Yaglom 1975). Also, among the evolved configurations, there is at least one which shows a clean classical, non-intermittent, K41 behaviour. While we strongly believe that these results on temporal intermittency are worth a further and deeper investigation we also stress how they clearly indicate that the *time component of intermittency* is a phenomenon which is often neglected and should be taken into account more seriously (see Kida & Ohkitani 1992 for a discussion about temporal intermittency from the analysis of energy spectra) when trying to draw conclusions about synthetic quantities like the probability distribution functions of three-dimensional turbulence.

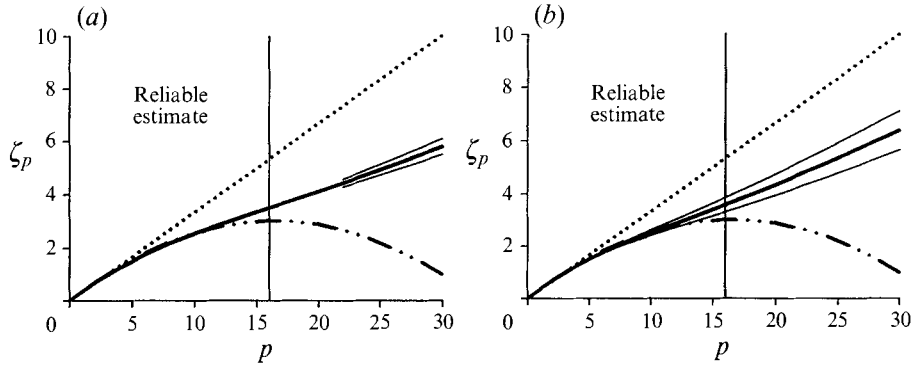

FIGURE 10. The same as in figure 9 but with the ζ_p exponents obtained by applying the *unweighted* (*a*) and the *weighted* (*b*) least-squares linear fit method, for the *p*th-order structure functions versus *r*, after the removal of the systematic fluctuating component due to the temporal intermittency of the system. Our numerical results are shown using a thick continuous line and errors are indicated by the $\pm 1\sigma$ confidence bounds (thin continuous lines). The K41 theory (Kolmogorov 1941) (· · ·), and the log-normal distribution (Monin & Yaglom 1975) (—··—) lines are shown for comparison. Note how the results are in agreement with those of figure 9 only inside the *reliable* range while they deviate appreciably outside, indicating an apparently smaller intermittency. The small errors of the estimate of the ζ_p exponents, inside the *non-reliable* range, is the result of the statistical analysis and has no physical meaning; in fact, this fictitious precision can be explained in terms of the the sampling cutoff shown in figure 7 and defined by formula (4.2) (see the text for a more detailed discussion).

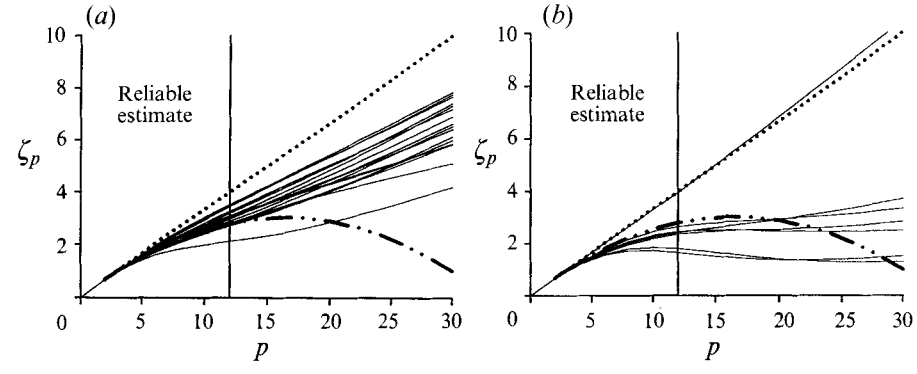

FIGURE 11. The same as in figure 10 but here the ζ_p exponents versus p are reported in detail for each of the 25 statistically independent configurations. The curves that best reproduce the *mean* behaviour are shown in (*a*) while (*b*) indicates the curves (corresponding to configurations 2, 7, 9, 12, 14 and 24), that loosely resemble the Kolmogorov–Obukhov log-normal model. Among the evolved states, in (*b*), configuration 6 shows a clean K41 behaviour. Note how the *temporal intermittency* does not allow one to identify a simple 'mean curve' but rather the curves can be grouped at least into two sets. Note also how the reduced number of available data per configuration (of the order of 3×10^5) shrinks the *reliable range* to $p < 12$ and still allows one to classify the configurations.

5. Conclusions

This paper reports the statistical analysis of the velocity field of a low-resolution (64^3) numerical simulation of fully developed homogeneous turbulence where the small scales are parametrized using the simple Kraichnan eddy-viscosity model. The results have indicated how (i) a clear $k^{-5/3}$ self-similar energy spectrum extends over a

wide extent of the resolved scales and is conserved during the entire simulation, (ii) the tails of PDFs of the velocity structure functions tend to an exponential behaviour for small scales and, (iii) the ζ_p power-law exponents of the velocity structure functions are in agreement with previous experimental and numerical data for $p \leqslant 16$. The third result is supported by the introduction of a reliable statistical criterion that allows one to select accurately which PDFs of the momenta of the structure functions, and which ζ_p exponents, can be measured reliably from the available data.

The use of this statistical criterion suggests that the spatial intermittency of the single configurations can be analysed in detail, without the need of time averaging in order to improve the statistics. We have applied this procedure to our numerical experiment and we have found some clues to the nature of its temporal intermittency. In particular, we have observed that, while most of the time the system shows a *mean* behaviour, there is a non-negligible set of configurations that exhibit a stronger spatial intermittency.

All these results confirm the validity of the large-eddy simulation method, even with a limited numerical resolution, as a tool to reproduce both the phenomenology and the main statistical properties of homogeneous turbulence.

The agreement of the results obtained using a low-resolution simulation with Kraichnan's eddy-viscosity model with those obtained from high-resolution direct simulations of turbulence (Vincent & Meneguzzi 1991), or from experimental data (Antonia *et al.* 1982), suggests that the statistics of homogeneous turbulence is essentially independent of the dissipative model used.

The authors wish to thank R. Benzi and G.F. Carnevale for useful comments and suggestions.

REFERENCES

ANSELMET, F. GAGNE, Y. HOPFINGER, E. J. & ANTONIA R. A. 1984 High-order velocity structure functions in turbulent shear flows. *J. Fluid Mech.* **140**, 63.

ANTONIA, R. A. SATYAPRAKASH, B. R. & HUSSAIN, A. K. M. F. 1982 Statistics of fine-scale velocity in turbulent plane and circular jets. *J. Fluid Mech.* **119**, 55.

BENZI, R., BIFERALE, L., PARISI, G., VULPIANI, A. & VERGASSOLA, M. 1991 Multifractality in the statistics of the velocity gradients in turbulence. *Phys. Rev. Lett.* **67**, 2302.

BRISCOLINI, M. & SANTANGELO, P. 1992 Numerical simulations of three-dimensional homogeneous isotropic flows. In *Proc. Conf. on Parallel Computing: Problems, Methods and Applications* (ed. P. Messina & A. Murli). Elsevier.

CASTAIGNE, B. GAGNE, Y. & HOPFINGER, E. J. 1990 Velocity probability density functions of high Reynolds number turbulence. *Physica* D, **46**, 177.

CHOLLET, J. P. & LESIEUR, M. 1981 Parameterization of small scales of three-dimensional isotropic turbulence utilizing spectral closure. *J. Atmos. Sci.* **38**, 2747.

FRISCH, U. & PARISI, G. 1985 On singularity structure of fully developed turbulence. In *Turbulence and Predictability in Geophysical Fluid Dynamics and Climate Dynamics* (ed. M. Ghil, R. Benzi, & G. Parisi), p. 84. North-Holland.

FRISCH, U. SULEM, P. L. & NELKIN, M. 1978 A simple dynamical model of intermittent fully developed turbulence. *J. Fluid Mech.* **87**, 719.

HOSOKAWA, I. & YAMAMOTO, K. 1990 Intermittency exponents and generalized dimensions of a directly simulated fully developed turbulence. *Phys. Fluids* A, **2**, 889.

KERR, R. 1985 Higher-order derivative correlations and the alignment of small-scale structures in isotropic numerical turbulence. *J. Fluid Mech.* **153**, 31.

KIDA, S. 1991 Log-stable distribution and intermittency of turbulence. *J. Phys. Soc. Japan.* **60**, 5.

KIDA, S. & MURAKAMI, Y. 1989 Statistics of velocity gradients at moderate Reynolds numbers. *Fluid Dyn. Res.* **4**, 347.

KIDA, S. & OHKITANI, K. 1992 Spatiotemporal intermittency and instability of a forced turbulence. *Phys. Fluids* A **4**, 1018.

KOLMOGOROV, A. N. 1941 Local structure of turbulence in an incompressible fluid at very high Reynolds numbers. *Dokl. Akad. Nauk. SSSR* **30**, 299.

KOLMOGOROV, A. N. 1962 A refinement of previous hypotheses concerning the local structure of turbulence in a viscous incompressible fluid at high Reynolds number. *J. Fluid Mech.* **13**, 82.

KRAICHNAN, R. H. 1974 On Kolmogorov's inertial-range theories. *J. Fluid Mech.* **62**, 305.

KRAICHNAN, R. H. 1976 Eddy viscosity in two and three dimensions. *J. Atmos. Sci.* **33**, 1521.

KRAICHNAN, R. H. 1990 Models of intermittency in hydrodynamic turbulence. *Phys. Rev. Lett.* **65**, 575.

LESIEUR, M. & ROGALLO, R. 1989 Large-eddy simulation of passive scalar diffusion in isotropic turbulence. *Phys. Fluids* A **1**, 718.

MANDELBROT, B. B. 1974 Intermittent turbulence in self-similar cascades: divergence of high moments and dimension of the carrier. *J. Fluid Mech.* **62**, 331.

MENEVEAU, C. & SREENIVASAN, K. R. 1987*a* The multifractal spectrum of the dissipation field in turbulent flows. *Nucl. Phys.* B *(Proc. Suppl.)*, **2**, 49.

MENEVEAU, C. & SREENIVASAN, K. R. 1987*b* The simple multifractal cascade model for fully developed turbulence. *Phys. Rev. Lett.* **59**, 1424.

MENEVEAU, C. & SREENIVASAN, K. R. 1991 The multifractal nature of turbulent energy dissipation. *J. Fluid Mech.* **224**, 429.

METAIS, O. & LESIEUR, M. 1992 Spectral large-eddy simulation of isotropic and stably stratified turbulence. *J. Fluid Mech.* **239**, 157.

MONIN, A. S. & YAGLOM, A. M. 1975 *Statistical Fluid Mechanics*, Vol.II. MIT Press.

OBUKHOV, A. M. 1962 Some specific features of atmospheric turbulence. *J. Fluid Mech.* **13**, 77.

ORSZAG, S. A. 1971 Numerical simulation of incompressible flows within simple boundaries. I. Galerkin (spectral) representation. *Stud. Appl. Maths* L, 293.

PRESS, W. H., FLANNERY, B. P., TEUKOLSKY, S. A. & VETTERLING, W. T. 1989 *Numerical Recipes*, Cambridge Univeristy Press.

SHE, Z.-S. 1991 Physical model of intermittency in turbulence: near-dissipation-range non-Gaussian statistics. *Phys. Rev. Lett.* **66**, 600.

SHE, Z.-S. & ORZSAG, S. A. 1991 Physical model of intermittency in turbulence: inertial-range non-gaussian statistics. *Phys. Rev. Lett.* **66**, 1701.

SREENIVASAN, K. R. & KAILASNATH, P. 1993 An update on the intermittency exponent in turbulence. *Phys. Fluids A* **5**, 512.

VINCENT, A. & MENEGUZZI, M. 1991 The spatial structure and statistical properties of homogeneous turbulence. *J. Fluids Mech.* **225**, 1.

YAKHOT, V. & ORSZAG, S. A. 1986 Renormalization group analysis of turbulence. I. Basic theory. *J. Sci. Comput.* **1**, 3.